

# Epitaxial growth and properties of $\text{MoO}_x$ ( $2 < x < 2.75$ ) films

V. Bhosle, A. Tiwari, and J. Narayan

*NSF Center for Advanced Materials and Smart Structures, Department of Materials Science & Engineering, North Carolina State University, Raleigh, North Carolina 27695-7916*

(Received 11 August 2004; accepted 13 January 2005; published online 11 April 2005)

We report the growth of epitaxial molybdenum oxide ( $\text{MoO}_x$ ,  $2 < x < 2.75$ ) films on  $c$  plane of sapphire substrate using pulsed laser deposition in oxygen environment. The structure was characterized using x-ray diffraction, high resolution transmission electron microscopy and x-ray photoelectron spectroscopy (XPS). Electrical resistivity and optical properties were investigated using four-point-probe resistivity measurements and spectroscopy techniques, respectively. It was found that the film had a monoclinic structure based on  $\text{MoO}_2$  phase and showed an unusual combination of high conductivity and high transmittance in the visible region after annealing. The unusual combination of these properties was realized by systematically controlling the relative fraction of different oxidation states of molybdenum, namely  $\text{Mo}^{4+}$ ,  $\text{Mo}^{5+}$ , and  $\text{Mo}^{6+}$  in the monoclinic phase. For a film 60 nm thick and annealed at 250 °C for 1 h, the ratio of  $\text{Mo}^{6+}/(\text{Mo}^{4+} + \text{Mo}^{5+})$  was determined to be  $\sim 2.9/1$  using XPS, and a typical value of transmittance was  $\sim 65\%$  and resistivity close to  $1 \times 10^{-3} \Omega \text{ cm}$ . These results demonstrate growth of epitaxial  $\text{MoO}_x$  films with tunable electrical and optical properties. Further optimization of these properties is expected to result in applications related to display panels, solar cells, chromogenic (photochromic, electrochromic, gasochromic) devices, and transparent conducting oxides. Our ability to grow epitaxial  $\text{MoO}_x$  films can further aid their integration with optoelectronic and photonic devices. © 2005 American Institute of Physics. [DOI: 10.1063/1.1868852]

## I. INTRODUCTION

Molybdenum oxide is a very interesting material and has found applications in a wide variety of fields such as optically switchable coatings,<sup>1,2</sup> gas sensors,<sup>3</sup> catalysis,<sup>4</sup> and also as diffusion barrier.<sup>5</sup> Molybdenum oxide exhibits electrochromism and photochromism after intercalating with an appropriate cation (such as  $\text{Li}^+$ ,  $\text{Na}^+$ ), making it suitable for their use in display devices, smart windows and storage batteries.<sup>6</sup> It also exhibits gasochromism and shows appreciable CO sensing capability, which makes these oxides a potential candidate for gas sensor applications.<sup>3,7</sup> The display of such varied properties is related to the existence of several different allotropes and phases of molybdenum oxides depending on the chemical composition and the formal oxidation state of molybdenum. Some of these compounds are  $\text{MoO}_3$  ( $\alpha$ - $\text{MoO}_3$  orthorhombic and  $\beta$ - $\text{MoO}_3$  monoclinic),  $\text{MoO}_2$  (monoclinic),  $\text{Mo}_4\text{O}_{11}$  (monoclinic, orthorhombic), and  $\text{Mo}_9\text{O}_{26}$  (triclinic, monoclinic), which show some very interesting electrical and optical properties as a function of oxygen vacancy concentration and nonstoichiometry.<sup>6-11</sup> The proper combination of some of these phases or a proper distribution of molybdenum ions with different oxidation states may lead to materials with superior electronic and optical properties. It is well known that  $\text{MoO}_3$  (Mo as  $\text{Mo}^{6+}$ ) is insulating and transparent,<sup>12</sup> whereas  $\text{MoO}_2$  (Mo as  $\text{Mo}^{4+}$ )<sup>10</sup> is a metallic conductor. Therefore, it has been conjectured that an appropriate mixture of these phases or these ions can form a material, which is transparent as well as conducting. Nonstoichiometric  $\text{MoO}_x$  films are an excellent candidate to study the effect of composition on the structure and properties of such films. Recently, there have been some reports

about the growth of  $\text{MoO}_x$  films consisting of mixed phases and molybdenum oxidation states by various deposition techniques.<sup>3,6,7,11</sup> These compounds have shown interesting physical properties, however, there have been no observations reported on a concomitant enhancement of transmittance and electrical conductivity. Previous studies on  $\text{MoO}_x$  films have also shown an ambiguity associated with the crystal structure of these materials. It has been reported that the film structure could be a single phase<sup>3,13</sup> or a mixture of several distinct molybdenum oxide phases with known structures.<sup>6</sup>

Molybdenum oxide films studied in the present work have a monoclinic structure where molybdenum exists in  $\text{Mo}^{4+}$ ,  $\text{Mo}^{5+}$ , and  $\text{Mo}^{6+}$  oxidation states. The most interesting observation is that the relative concentration of  $\text{Mo}^{4+}$ ,  $\text{Mo}^{5+}$ , and  $\text{Mo}^{6+}$  in the film can be varied with annealing and  $x$  in  $\text{MoO}_x$  is adjusted accordingly, while still retaining the basic crystal structure. The molybdenum oxide ( $\text{MoO}_x$ ) films were deposited using pulsed laser deposition (PLD) in oxygen environment and characterized to determine the structure and composition. The physical properties such as optical absorption and electrical resistivity were measured and the effect of annealing on the variation of these properties was studied. Correlations between structure, chemical composition, and electrical and optical properties of the films were also investigated. Finally, the potential of these  $\text{MoO}_x$  films for applications in several chromogenic devices, solar cells, display panels and as transparent conducting oxide is discussed.

## II. EXPERIMENT

$\text{MoO}_x$  films were grown on  $c$ -plane sapphire single crystal substrates by pulsed laser deposition.<sup>14</sup> Molybdenum

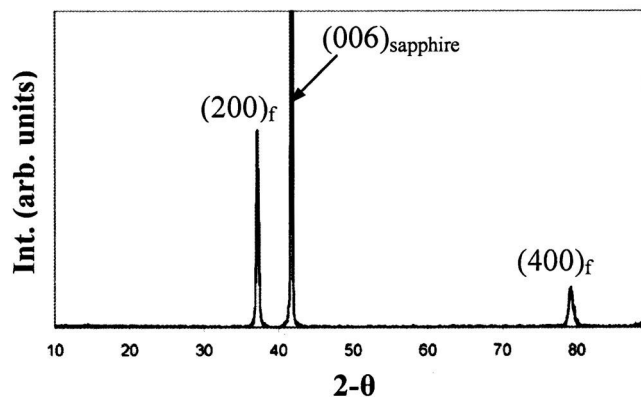


FIG. 1. XRD pattern of the film (*f*) in as deposited condition.

metal (99.9%) and molybdenum dioxide ( $\text{MoO}_2$ ) targets used for deposition were obtained from H. C. Starck, Inc. A pulsed KrF excimer laser with a wavelength of 248 nm was used for ablation. The energy density of the laser beam was varied from 4 to 7 J/cm<sup>2</sup> with a repetition rate of 10 Hz. The chamber was evacuated to a base pressure of  $6 \times 10^{-7}$  Torr and the deposition was carried out at  $1 \times 10^{-3}$  Torr of oxygen pressure. The deposition was performed in the temperature range of 500–600 °C for 15 min. Films were deposited using a compound assembly consisting of Mo metal and  $\text{MoO}_2$  target. Films were also annealed at 250 °C for different durations of time to investigate the effect of heating on their optical and electrical properties. X-ray diffraction (XRD) of the films was carried out using Rigaku x-ray diffractometer with Cu  $K\alpha$  radiation ( $\lambda = 1.54 \text{ \AA}$ ) and a Ni filter. JEOL-2010 field emission transmission electron microscope (TEM) attached to Gatan image filter was used to perform the structural characterization of the film. X-ray photoelectron spectroscopy (XPS) was performed using Riber LAS-3000 instrument with Mg  $K\alpha$  x-ray source. An analysis of different oxidation states from the spectrum with overlapping peaks was performed by deconvolution using Shirley routine and Casa software. The values corresponding to C 1s peak were used as reference for the curve fitting analysis. Optical measurements (absorption/transmission) were made using an Hitachi: U-3010 spectrophotometer while the electrical resistivity was measured using the four-point-probe technique.

### III. RESULTS AND DISCUSSION

#### A. Structural characterization

Figure 1 shows the XRD ( $\theta$ - $2\theta$  scan) of the film in the as-deposited condition which suggests the formation of a highly oriented film consisting of a single phase. Further analysis of the structure of the films was carried out using electron diffraction and high-resolution transmission electron microscopy (HRTEM) Figure 2 is a low magnification image of the as-deposited  $\text{MoO}_x$  film on sapphire. From the cross-section TEM micrograph the thickness of the film was determined to be 60 nm. The structure was determined using the diffraction pattern taken in  $[001]_f$  and  $[010]_f$  direction. Figures 3(a) and 3(b) are the selected area electron diffraction (SAED) of the film corresponding to the zones  $[001]_f$  and

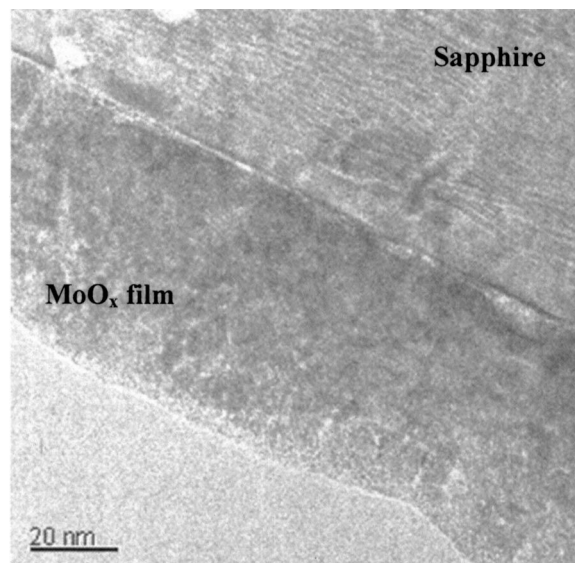


FIG. 2. Low magnification image the film on sapphire.

$[010]_f$ , respectively. It can be seen from Figs. 3(a) and 3(b) that a single-phase film has grown epitaxially on the (0001) sapphire substrate. From the diffraction patterns in Fig. 3, the phase is identified to be  $\text{MoO}_2$  with a monoclinic structure, which is consistent with the earlier observations.<sup>15–17</sup> The lattice parameters from the diffraction (electron and XRD) patterns, were determined to be,  $a = 5.610 \pm 0.01 \text{ \AA}$ ,  $b = 4.856 \pm 0.01 \text{ \AA}$ ,  $c = 5.628 \pm 0.01 \text{ \AA}$  and  $\beta \approx 120.6^\circ \pm 0.1^\circ$  which are in good agreement with the values reported previously.<sup>17</sup> Thus, for a monoclinic structure with these lattice parameters, the diffraction observed in  $[001]$  zone (i.e.,  $a^*b^*$  plane) is a square pattern since the angle between  $a^*$  and  $b^*$  is  $90^\circ$ , while in  $[010]$  zone (i.e.  $a^*c^*$  plane), a hexagonal pattern is observed as angle between  $a^*$  and  $c^*$  is close to  $60^\circ$ .<sup>16</sup> Figure 3(c) shows the SAED at the interface depicting the orientation relationship between the substrate and the epitaxial film as follows:  $(200)_f \parallel (0006)_s$  (out of plane) and  $[001]_f \parallel [01\bar{1}0]_s$  (in plane). The  $d$  spacing measured for (200) planes from the electron diffraction also corresponds to the XRD peak observed at  $2\theta = 37.2^\circ$ , thus confirming the (200) orientation of the film.  $\text{MoO}_x$  films grow epitaxially on sapphire by domain matching epitaxy where integral multiples of lattice planes match across the film-substrate interface.<sup>18</sup> In the present case, the misfit between the planar spacings across the interface is only  $\sim 1.2\%$  and every one plane of substrate matches with one plane of the film. Interestingly, along  $[01\bar{1}0]$ , the mismatch between the planar spacings of substrate and the film is also  $\sim 1.1\%$ . This lattice mismatch is accommodated by (1/1) matching of planes (i.e., one plane of sapphire with  $d = 2.748 \text{ \AA}$ , match with one plane of the film having  $d = 2.78 \text{ \AA}$ ). The additional misfit is accommodated by the principle of domain variation, whereby the domain repeats with a certain frequency to reduce the total misfit close to zero. Figure 4 is a HRTEM image of the  $\text{MoO}_x$ /sapphire interface in  $[001]$  zone of the film. The interface is observed to be sharp without any noticeable interfacial reaction, which might have facilitated the epitaxial growth of the film. The HRTEM image also shows

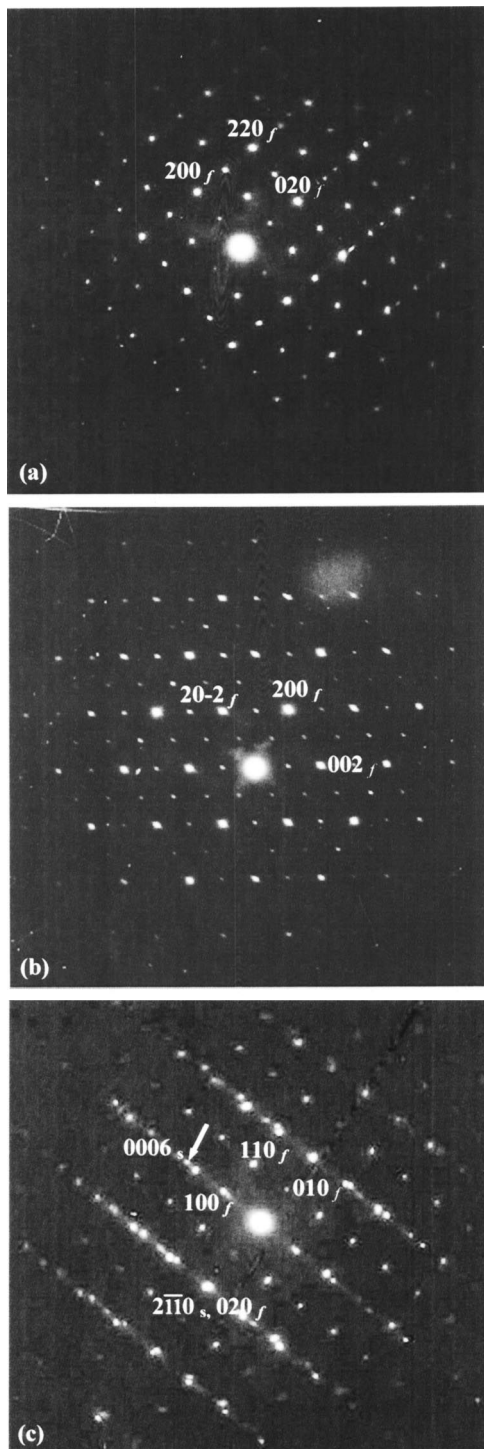


FIG. 3. (a) SAED of the film in [001] zone, (b) SAED of the film in [010] zone. (c) SAED of the interface.

the square arrangement of atomic columns in the film, characteristic of the image of the crystal when viewed along the  $c$  axis.

In the abovementioned monoclinic phase, molybdenum is present as  $\text{Mo}^{4+}$ ,  $\text{Mo}^{5+}$ , and  $\text{Mo}^{6+}$  along with oxygen vacancies, depending on the annealing condition. The presence of the different molybdenum species ( $\text{Mo}^{4+}$ ,  $\text{Mo}^{5+}$ —metallic and  $\text{Mo}^{6+}$ ) in the  $\text{MoO}_x$  film has been verified by XPS. Figure 5(a) is the XPS survey spectrum acquired from surface of the as deposited  $\text{MoO}_x$  film, which shows the peaks corre-

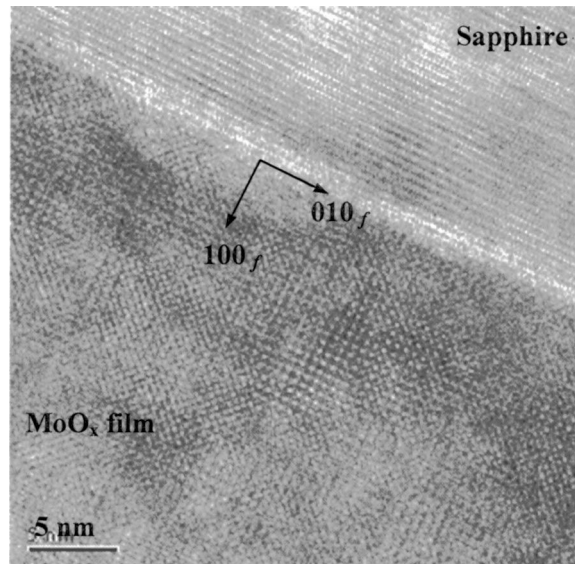


FIG. 4. HRTEM of the interface.

sponding to Mo 3d, O 1s and C 1s and does not indicate the presence of any extra elements. The high-resolution Mo 3d core level spectrum of the film in as deposited condition is presented in Fig. 5(b). The observed spectrum is characteristic of the complex mixture of Mo  $3d_{5/2,3/2}$  spin doublets of molybdenum in its oxidation state of +4, +5, and +6.<sup>13,19</sup> A nonlinear curve fitting program has been used to resolve the  $\text{Mo}^{4+}$  ( $3d_{5/2}$ ) peak observed at 229.7 eV, while  $\text{Mo}^{6+}$  ( $3d_{5/2}$ ) peak at 232.6 eV. In addition to the presence of  $\text{Mo}^{4+}$  and  $\text{Mo}^{6+}$  states, there also exists a small amount of molybdenum in the  $\text{Mo}^{5+}$  valence state. The  $3d_{5/2}$  peak corresponding to the  $\text{Mo}^{5+}$  state is observed at 231.1 eV. Figure 5(b) also shows a simulated spectra (constructed using Shirley fitting routine) for peaks corresponding to  $3d_{5/2,3/2}$  spin doublets of  $\text{Mo}^{4+}$ ,  $\text{Mo}^{5+}$ , and  $\text{Mo}^{6+}$  states. The observed peak positions are in accordance with the values reported in the literature.<sup>2,13,19</sup> The relative concentration of each species ( $\text{Mo}^{4+}$ ,  $\text{Mo}^{5+}$ , and  $\text{Mo}^{6+}$ ) was determined by calculating the area under the resolved peaks. It was found that the ratio of ( $\text{Mo}^{4+} + \text{Mo}^{5+}$ ) and  $\text{Mo}^{6+}$  was  $\sim 2.1:1$ , in the as deposited condition.

## B. Effect of annealing

### 1. Effect on structure and composition

Figure 6(a) shows XRD of the films annealed for different durations of time and it can be seen from the XRD patterns that the structure does not change even after annealing the films for 8 h. This has also been verified from the electron diffraction of the film annealed at 250 °C for 1 h as shown in Fig. 6(b). Annealing, however, changes the oxygen stoichiometry considerably. The high-resolution Mo 3d core level spectrum of the film annealed at 250 °C for 1 h is presented in Fig. 7 and the ratio of ( $\text{Mo}^{4+} + \text{Mo}^{5+}$ ) and  $\text{Mo}^{6+}$  was determined to be  $\sim 1:2.9$ . The increase in the  $\text{Mo}^{6+}$  state after annealing in air can be explained by the oxidation of the film. During annealing, these vacant sites are filled with oxygen atoms, changing the oxidation state of molybdenum to  $\text{Mo}^{6+}$ , while still retaining the original crystal structure.<sup>20</sup>

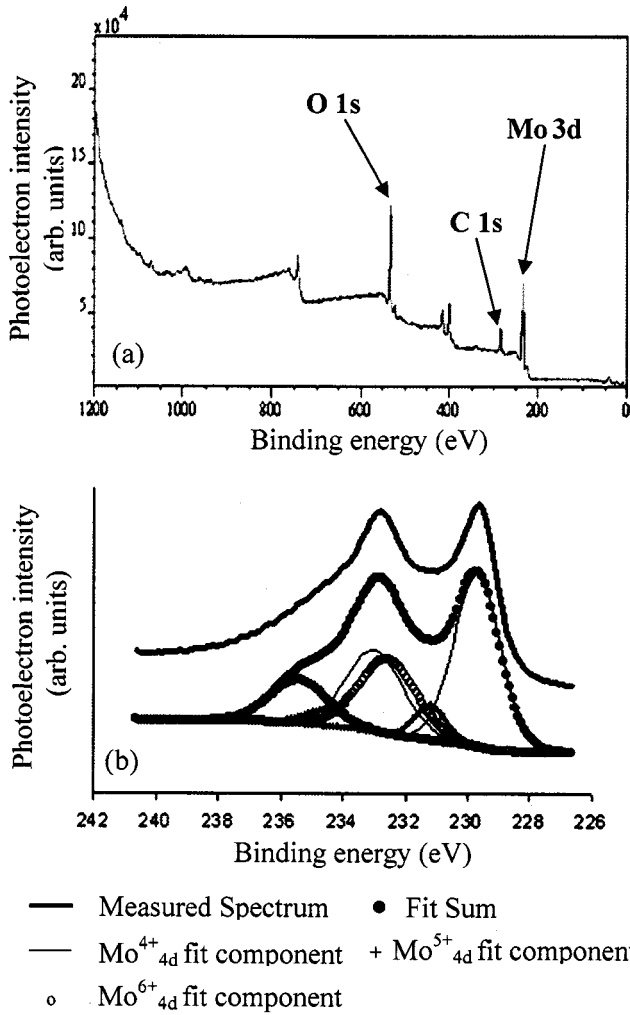


FIG. 5. (a) Survey XPS spectrum from the surface of the film in the as deposited condition. (b) High-resolution spectrum of the as deposited film.

Earlier reports on oxidation of MoO<sub>2</sub> or reduction of MoO<sub>3</sub> films suggest the formation of intermediate phases, e.g., Mo<sub>4</sub>O<sub>11</sub>, Mo<sub>8</sub>O<sub>23</sub>, Mo<sub>9</sub>O<sub>26</sub>, and Mo<sub>18</sub>O<sub>52</sub>.<sup>21,22</sup> However, no such phase was detected by XRD or TEM during annealing of these films. Thus it appears that the oxidation primarily involves the movement of oxygen atoms and only limited movement of Mo. This is reasonable because the change of structure will require higher activation energy for Mo atoms as compared to oxygen. The oxygen atoms can diffuse by interstitial diffusion mechanism at low annealing temperature (~250 °C). The diffusion can also be retarded due to lack of the defects in epitaxial films, which could further restrict the motion of Mo atoms. However, the stability of the structure also limits the extent of the oxidation of the films and, thus, the corresponding change in properties. Under equilibrium conditions of oxidation, Mo<sub>4</sub>O<sub>11</sub> phase will form if oxygen concentration exceeds 73.33%. However, since formation of Mo<sub>4</sub>O<sub>11</sub> was not observed, it can be assumed that 73.33% of oxygen is an approximate limit during oxidation and the films cannot be oxidized further without changing the structure. Annealing also affects the optical and electrical properties of the films, as described in the section below.

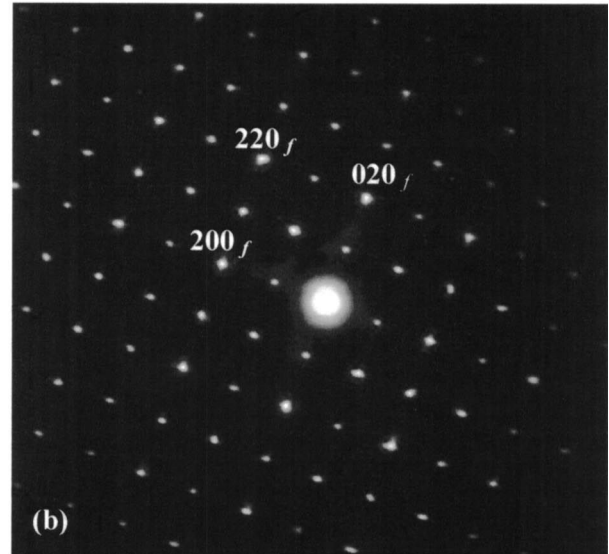
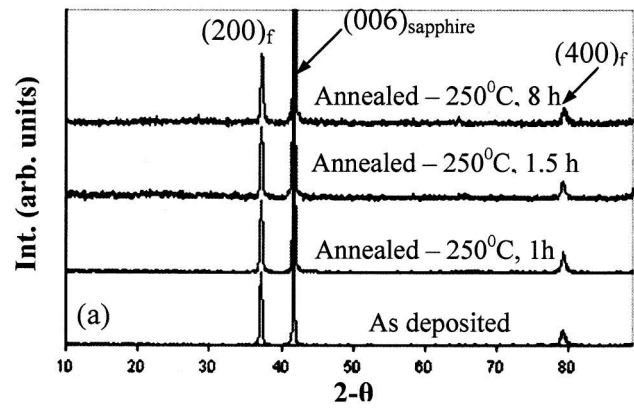


FIG. 6. (a) XRD pattern of the film in as deposited condition and after annealing. (b) SAED of the film annealed at 250 °C for 1 h in [001] zone.

## 2. Effect on optical and electrical properties

Figure 8 compares the results of absorption and transmittance measurements performed on 60-nm-thick films, deposited at 550 °C and annealed at 250 °C for different intervals of time. The transmittance of the film in the visible wavelength region strongly depends on the annealing conditions and it increases as the annealing time increases. The maximum absorption occurs in the wavelength range of 350–450 nm which is in agreement with the observations reported in previous studies.<sup>9,12</sup> The absorption edge moves toward lower wavelength, which suggests the slight increase in the band gap of the material. However, since the absorption edge is broad, exact determination of the band gap from the absorption spectrum was difficult. Nevertheless, it is evident from these spectra that the transmittance of the film can be increased appreciably by annealing the films in air. Another observation is the decrease in the electrical conductivity of the films with annealing time. Table I summarizes the annealing conditions, %*T*, the corresponding resistivity, and the ratio of (Mo<sup>4+</sup>+Mo<sup>5+</sup>)/Mo<sup>6+</sup> in these films.

The as deposited molybdenum oxide films are substoichiometric and contain a large number of vacancies, and lower oxidation states of molybdenum such as Mo<sup>4+</sup> and Mo<sup>5+</sup> which lead to increased absorption and electrical con-

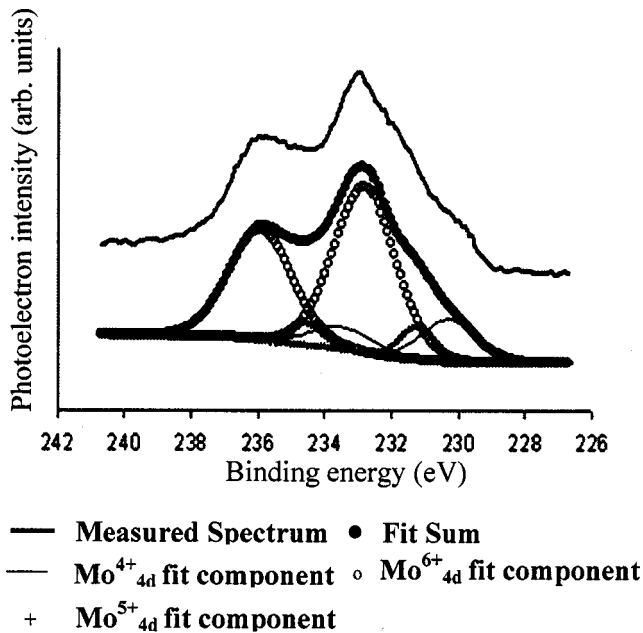
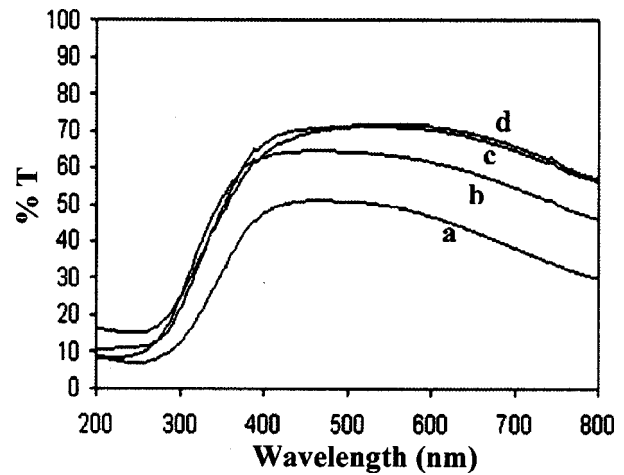


FIG. 7. High-resolution spectrum of the film annealed at 250 °C for 1 h.

ductivity. Thus, the conductivity can be ascribed to the presence of lower valence states of Mo and oxygen vacancies. It has also been suggested that in molybdenum oxide, the valence band is occupied by the O 2*p* states, while the conduction band has contribution from Mo 4*d* states.<sup>13</sup> However, the nature of 4*d* states (i.e., the bonding and electron sharing) is different when molybdenum is in Mo<sup>4+</sup> and Mo<sup>6+</sup> valence state. This could further lead to changes in electronic band structure of the material and influence the physical properties of the films.

The observed increase in the transmittance and resistivity during annealing can be explained by the occupancy of vacant sites by oxygen and the change in fraction of Mo oxidation states during annealing. In the case of annealed films electrical conduction can occur by the hopping-electron mechanism between different oxidation states ( $e^-$  moving from Mo<sup>4+</sup> → Mo<sup>5+</sup> → Mo<sup>6+</sup>).<sup>12</sup> The oxidation of MoO<sub>x</sub> film converts Mo<sup>4+</sup> to Mo<sup>6+</sup> and also reduces the oxygen vacancy concentration, thus increasing the transmittance and resistivity of the film. This is in good agreement with XPS results, which confirm the increase of Mo<sup>6+</sup> states after annealing [Figs. 5(b) and 7]. However, as described in the previous

FIG. 8. Optical transmittance of the MoO<sub>x</sub> films. (a) As deposited, (b) annealed -250 °C, 1 h, (c) annealed -250 °C, 1.5 h, (d) annealed -250 °C, 8 h.

section, the oxidation of the films is limited and so is the increase in the Mo<sup>6+</sup> fraction and consequent change in its properties. It can be seen from the transmittance data (Fig. 8) that the %*T* does not increase significantly beyond ~70%. Though, %*T* increases with annealing time for films annealed up to 1.5 h, no notable change is observed in transmittance of the films annealed for more than 1.5 h, even in films annealed up to 8 h. This is in agreement with the supposition that the oxidation of the films is limited and, therefore, the transmittance cannot be increased beyond a certain value without changing the structure. Thus, any further increase in transmittance would require higher annealing temperature enabling further oxidation of the films and possibly alteration of structure.

From the study it was found that the film annealed at 250 °C for 1 h showed the transmittance of ~65% and the room temperature resistivity equal to  $1 \times 10^{-3} \Omega \text{ cm}$  and the corresponding ratio of (Mo<sup>4+</sup>+Mo<sup>5+</sup>):Mo<sup>6+</sup> was found to be ~1/2.9 (25.6%, 74.4%). Figure 9 is the plot of resistivity as a function of temperature for the same film, and the value of resistivity measured is much lower than that reported for amorphous substoichiometric molybdenum oxide, which is almost insulating.<sup>12</sup> It can also be observed that the film shows metallic behavior with a temperature coefficient of resistivity  $\sim 0.0129 \times 10^{-4} \Omega/\text{K}$ . These results show a possi-

TABLE I. Summary of annealing conditions and optical and electrical properties and the corresponding fraction of different molybdenum oxidation states in the MoO<sub>x</sub> films.

Sample	Annealing conditions		%T (±5%)	RT resistivity (Ω cm)	~% Mo <sup>4+</sup>	~% Mo <sup>5+</sup>	~% Mo <sup>6+</sup>	(Mo <sup>4+</sup> +Mo <sup>5+</sup> ): Mo <sup>6+</sup>
	Temperature	Holding time						
As-deposited	...	...	47.7	$7.2 \times 10^{-5}$	60.00	8.31	31.71	2.1:1
Annealed 1	250 °C	1 h	65.1	$1.0 \times 10^{-3}$	17.09	8.40	74.50	1:2.9
Annealed 2	250 °C	1.5 h	71.5	$1.5 \times 10^{-2}$	...	...	...	...

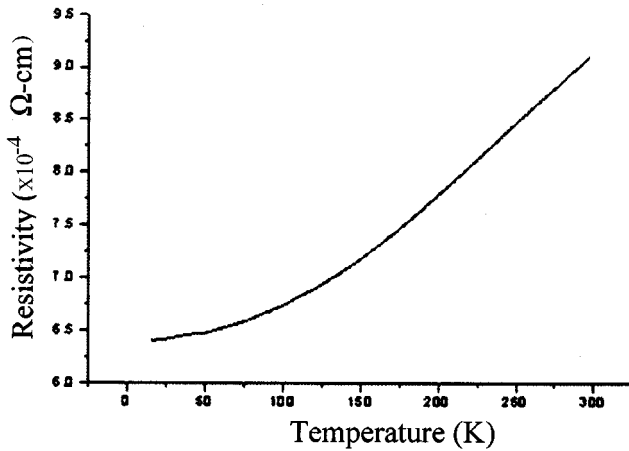


FIG. 9. Plot of resistivity as a function of temperature.

bility of using these films as transparent conducting oxide (TCO). However, the values reported here for %*T* and resistivity are certainly not close to those of commercially available indium tin oxide (ITO) (%*T* > 80,  $\rho \sim 10^{-4} \Omega \text{ cm}$ ) which is currently used for TCO applications. Nevertheless,  $\text{MoO}_x$  films should exhibit superior diffusion characteristics<sup>5</sup> compared to ITO, and optimization of processing conditions should further enhance the properties of the films. This will probably be another application for the epitaxial  $\text{MoO}_x$  films in addition to its known applications, such as its use in Li batteries and in several other chromogenic devices. In addition, the ability to grow epitaxial  $\text{MoO}_x$  films on sapphire can also aid their integration with optoelectronic and photonic devices. This work shows that the properties of the  $\text{MoO}_x$  films can be easily altered by annealing in air and also optimized to achieve desired value of transmittance and electrical conductivity depending upon the applications. However, since oxidation is a diffusion-based process and proceeds from surface to interior, it is cautioned here that the effectiveness of annealing in altering the film properties can be strongly affected by its thickness. Although, at this stage the effect of thickness on the physical properties of these films has not been studied, it should be interesting to investigate this in future.

#### IV. SUMMARY

Single crystal  $\text{MoO}_x$  films were grown epitaxially on *c* plane of sapphire substrate, via domain matching epitaxy using PLD in oxygen environment. The thickness of the films was found to be in the range of 60 nm. The structural characterization revealed that films had (100) orientation and a monoclinic structure, where molybdenum exists in different oxidation states (i.e.,  $\text{Mo}^{4+}$ ,  $\text{Mo}^{5+}$ , and  $\text{Mo}^{6+}$ ). The film properties such as optical absorption and resistivity were systematically studied and it was found that by annealing in air, these properties could be easily altered without changing the structure. It was established that the properties were dependent on the concentration of oxygen vacancies, and relative concentrations of  $\text{Mo}^{4+}$ ,  $\text{Mo}^{5+}$ , and  $\text{Mo}^{6+}$  states in the film, which are changed during annealing. The films annealed at

250 °C for 1 h showed an unusual combination of high transmittance of  $\sim 65\%$  and electrical resistivity in the range  $1 \times 10^{-3} \Omega \text{ cm}$  and the relative concentration of  $\text{Mo}^{4+}$ ,  $\text{Mo}^{5+}$  and  $\text{Mo}^{6+}$  states was determined to be  $\sim 17.2\%$ ,  $\sim 8.4\%$ , and  $\sim 74.4\%$ , respectively. The presence of the different valence states of molybdenum ( $\text{Mo}^{4+}$ ,  $\text{Mo}^{5+}$ , and  $\text{Mo}^{6+}$ ) in  $\text{MoO}_x$  films was verified by XPS. Thus, we have shown that the presence of mixed Mo valence states in the  $\text{MoO}_x$  films can give rise to interesting optical and electrical properties which can be further controlled by the annealing conditions.

These results suggest the possibility of growing the epitaxial  $\text{MoO}_x$  films with easily tunable electrical and optical properties. The change of properties, however, does not alter the structure and could be an attractive feature for the application of  $\text{MoO}_x$  films in solid-state devices. Further work is needed to investigate the processing conditions to optimize the optical and electrical properties of the  $\text{MoO}_x$  films for their use in chromogenic (photochromic, electrochromic, gasochromic) devices, and also as TCOs. Related topics of interest will be to understand the electronic band structure of these  $\text{MoO}_x$  films and also probe into the oxidation process in detail.

#### ACKNOWLEDGMENTS

The authors are grateful to Fred Stevie for his help in XPS analysis and A. Chugh and H. Zhou for their assistance in TEM. We acknowledge partial support of H. C. Starck, Inc. and contributions of R. Wu and P. Kumar.

- <sup>1</sup>N. Miyata and S. Akiyoshi, *J. Appl. Phys.* **58**, 1651 (1985).
- <sup>2</sup>R. J. Colton, A. M. Guzman, and J. W. Rabalais, *J. Appl. Phys.* **49**, 409 (1978).
- <sup>3</sup>S. H. Mohamed, O. Kappertz, J. M. Ngaruiya, T. P. L. Pedersen, R. Drese, and M. Wuttig, *Thin Solid Films* **429**, 135 (2003).
- <sup>4</sup>W. Zhang, A. Desikan, and S. T. Oyama, *J. Phys. Chem.* **99**, 14468 (1995).
- <sup>5</sup>E. Kolawa, C. W. Nieh, F. C. T. So, and M. A. Nicolet, *J. Electron. Mater.* **17**, 425 (1988).
- <sup>6</sup>H. Ohtsuka and Y. Sakurai, *Jpn. J. Appl. Phys., Part 1* **40**, 4680 (2001).
- <sup>7</sup>J. Okumu, F. Koerfer, C. Salinga, and M. Wuttig, *J. Appl. Phys.* **95**, 7632 (2004).
- <sup>8</sup>P. F. Garcia and E. M. McCarron, *Thin Solid Films* **155**, 53 (1987).
- <sup>9</sup>M. Anwar and C. A. Hogarth, *Phys. Status Solidi A* **109**, 469 (1988).
- <sup>10</sup>M. A. K. L. Dissanayake, and L. L. Chase, *Phys. Rev. B* **18**, 6872 (1978).
- <sup>11</sup>M. A. Camacho-Lopez, L. Escobar-Alarcon, E. Haro-Poniatowski, *Appl. Phys. A: Mater. Sci. Process.* **78**, 59 (2004).
- <sup>12</sup>C. Julien, A. Khelifa, O. M. Hussain, and G. A. Nazri, *J. Cryst. Growth* **156**, 235 (1995).
- <sup>13</sup>O. Yu. Khyzhun, T. Strunkus, and Yu. M. Solonin, *J. Alloys Compd.* **366**, 54 (2004).
- <sup>14</sup>D. B. Chrisey and G. H. Hubler, *Pulsed Laser Deposition of Thin Films* (Wiley, New York, 1994).
- <sup>15</sup>B. G. Brandt and A. C. Skapski, *Acta Chem. Scand.* (1947-1973) **21**, 661 (1967).
- <sup>16</sup>Y. Gotoh and E. Yanokura, *Surf. Sci.* **287**, 279 (1993).
- <sup>17</sup>A. A. Bolzan, B. J. Kennedy, and C. J. Howard, *Banach Cent Publ.* **48**, 1473 (1995).
- <sup>18</sup>J. Narayan and B. C. Larson, *J. Appl. Phys.* **93**, 278 (2003).
- <sup>19</sup>P. A. Spevack and N. S. McIntyre, *J. Phys. Chem.* **96**, 9029 (1992).
- <sup>20</sup>G. Svensson and L. Kihlberg, *React. Solids* **3**, 33 (1987).
- <sup>21</sup>T. Ressler, J. Wienold, R. E. Jentoft, and T. Neisius, *J. Catal.* **210**, 67 (2002).
- <sup>22</sup>T. Ressler, R. E. Jentoft, J. Wienold, M. M. Gunter, and O. Timpe, *J. Phys. Chem. B* **104**, 6360 (2000).